IMMUNE NETWORK

Original Article

Check for updates

*Correspondence to
Moon Gyo Kim
Department of Biological Sciences, Inha University, 100 Inha-ro, Nam-gu, Incheon 22212, Korea.
E-mail: mgkim@inha.ac.kr

ORCID iDs
Ki Yeon Kim
https://orcid.org/0000-0002-8575-7680
Eun Hye Cho
https://orcid.org/0000-0001-7752-4441
Minsang Yoon
https://orcid.org/0000-0001-8828-1510
Moon Gyo Kim
https://orcid.org/0000-0002-3012-953X

Conflict of Interest
The authors declare that they have no conflicts of interest.

Abbreviations
alum-loop, mice immunized with loop metavaccine and alum; CFA-loop, mice immunized with loop metavaccine and Freund's complete adjuvant; CFA, Freund's complete adjuvant; DEG, Differentially

Critical Adjuvant Influences on Preventive Anti-Metastasis Vaccine Using a Structural Epitope Derived from Membrane Type Protease PRSS14

Ki Yeon Kim (ID)**, Eun Hye Cho** (ID)**, Minsang Yoon** (ID)**, Moon Gyo Kim** (ID)*

Department of Biological Sciences, Inha University, Incheon 22212, Korea

ABSTRACT

We tested how adjuvants effect in a cancer vaccine model using an epitope derived from an autoactivation loop of membrane-type protease serine protease 14 (PRSS14; loop metavaccine) in mouse mammary tumor virus (MMTV)-polyoma middle tumor-antigen (PyMT) system and in 2 other orthotopic mouse systems. Earlier, we reported that loop metavaccine effectively prevented progression and metastasis regardless of adjuvant types and T_H types of hosts in tail-vein injection systems. However, the loop metavaccine with Freund's complete adjuvant (CFA) reduced cancer progression and metastasis while that with alum, to our surprise, were adversely affected in 3 tumor bearing mouse models. The amounts of loop peptide specific antibodies inversely correlated with tumor burden and metastasis, meanwhile both T_H1 and T_H2 isotypes were present regardless of host type and adjuvant. Tumor infiltrating myeloid cells such as eosinophil, monocyte, and neutrophil were asymmetrically distributed among 2 adjuvant groups with loop metavaccine. Systemic expression profiling using the lymph nodes of the differentially immunized MMTV-PyMT mouse revealed that adjuvant types, as well as loop metavaccine can change the immune signatures. Specifically, loop metavaccine itself induces T_H2 and T_H17 responses but reduces T_H1 and T_{reg} responses regardless of adjuvant type, whereas CFA but not alum increased follicular T_H response. Among the myeloid signatures, eosinophil was most distinct between CFA and alum. Survival analysis of breast cancer patients showed that eosinophil chemokines can be useful prognostic factors in PRSS14 positive patients. Based on these observations, we concluded that multiple immune parameters are to be considered when applying a vaccine strategy to cancer patients.

Keywords: Adjuvant; metastasis; vaccine; PRSS14; breast cancer

INTRODUCTION

Tumor growth and metastasis are controlled by reprogramming tumor cells and tumor microenvironment (1). During immunoediting of tumors, both antigen-specific immune responses and general innate responses have important roles (2). During the 3 phases of immunoediting (elimination, equilibrium, and escape), various immune cells respond to tumor signals and modify the outcome of tumor progression. Typically, CD4⁺T, CD8⁺T,

Generated by xmlinkpress

expressed gene; id, identity; IFA, Freund's incomplete adjuvant; KLH, Keyhole limpet hemocyanin; MAL, polyoma middle tumor-antigen mice injected with loop metavaccine plus alum; MAP, polyoma middle tumor-antigen mice injected with alum without loop metavaccine; MCL, polyoma middle tumor-antigen mice injected with loop metavaccine plus Freund's complete adjuvant; MCP, polyoma middle tumor-antigen mice injected with Freund's complete adjuvant without loop metavaccine; MNI, polyoma middle tumor-antigen mice without any immunization; MMTV, mouse mammary tumor virus; PRSS14, serine protease 14; PyMT, polyoma middle tumor-antigen; ST14, suppression of tumorigenicity 14; TCGA, The Cancer Genome Atlas; TFH, follicular helper T cell; WAL, wild-type mice vaccinated with loop metavaccine plus alum; WAP, wild-type mice injected with alum; WCL, wild-type mice vaccinated with loop metavaccine plus Freund's complete adjuvant; WCP, wild-type mice injected with Freund's complete adjuvant; WNI, FVB wild-type mice without any vaccination.

macrophages (M1 and M2), neutrophils, monocytes, and eosinophils can act as anti-tumor or pro-tumor cell types depending on the circumstance (3,4).

Among the CD4$^+$ T_H subsets, it was suggested that T_H1, T_H2, and T_H17 have important roles in responses against cancers. To destroy tumors, T_H1 cells can activate cytotoxic T cells and recruit NK cells and M1 macrophages to tumor sites, whereas T_H2 cells activate B cells and recruit innate immune cells such as eosinophil (5). However, T_H2 cells can also promote tumor progression (6). The roles of T_H17 cells in the tumor microenvironment are also contradictory as they can promote angiogenesis and tumor growth or promote anti-cancer immunity (6). Follicular helper T cells (T_{FH}), which help B cells generate antigen-specific Abs (7), have roles in anti-tumor activity, while T_{reg} generally promote cancer progression (5). Therefore, it is helpful to understand the overall immune editing phenomenon by investigating the T_H signatures in the tumor bearing hosts.

Typically, adjuvants are compounds that enhance the quality, potency and longevity of antigen-specific immune responses. Freund's complete adjuvant (CFA), a water-in-oil emulsion containing inactivated mycobacteria, generally appears to induce a T_H1 type immune response (8,9). In addition, Freund's incomplete adjuvant (IFA) without mycobacteria, together with CFA can induce effective T_H1 and T_H2 type immune responses (8). While CFA is still widely used in animal experiments, it is considered too reactogenic for use in humans (10). Alum is currently the most commonly used adjuvant in human vaccines (10). However, the method by which alum modifies the immune system has not been fully understood. It is shown to induce a strong T_H2 immune response (9,11) and is also linked to serious autoimmune outcomes and adverse effects including association with breast cancer induction (12,13).

Serine protease 14 (PRSS14), also called epithin (14), matriptase (15), or membrane-type serine protease 1 (16), is a typical membrane-type serine protease that is overexpressed in multiple cancer cell lines and breast cancer tissues (17,18). Its role in breast cancer progression has been demonstrated in several conventional pathologic studies (19-21). When Prss14 hypomorphic mice, which express a minimal amount of Prss14, were crossed into spontaneous breast cancer transgenic mice, mouse mammary tumor virus (MMTV)-polyoma middle tumor-antigen (PyMT), tumor growth was significantly reduced (22). When breast cancer cell lines with Prss14 knocked down were implanted into syngeneic mouse strains, tumor growth and metastasis were reduced (9,23). In addition, the survival of patients that highly express PRSS14 (suppression of tumorigenicity 14 [ST14]) was remarkably low, especially in estrogen receptor negative (ER$^-$) or triple negative breast cancer patients (21).

To be a fully functional protease, Prss14 requires cleavage at its activation loop. Since Prss14 is capable of autoactivation, it can lead to activation of multiple downstream substrates (24,25). Recently, we reported that a structural epitope derived from a functionally important motif in the autoactivation loop of Prss14 can behave as an effective preventive metastasis vaccine (i.e., loop metavaccine) in 2 mouse models (9). Immunization of loop metavaccine increased the survival rate and decreased lung metastasis in tail-vein injection of E0771 or 4T1 into syngenic C57BL/6 (T_H1) or Balb/c (T_H2) hosts, respectively. In addition, injection of a monoclonal anti-loop Ab can abolish metastasis in tumor-bearing PyMT mice. However, the effects of loop metavaccine in spontaneous breast cancer or orthotopic models were not included in our previous studies.

We investigated the anti-metastasis effects of loop metavaccine with CFA and alum in 3 breast cancer mouse models in this study. By analyzing Ab production, tumor infiltrating cells, and systemic bioinformatics, we show that the anti-metastasis effect is due to high Ab levels and the presence of tumor infiltrating eosinophils. The importance of eosinophil chemotaxis in the immunological targeted therapy in a cancer vaccine approach is also described.

MATERIALS AND METHODS

Cells
The 4T1 cells were maintained in DMEM (Welgene, Gyeongsan, Korea) containing HEPES (Sigma, St. Louis, MO, USA), while the E0771 cells were maintained in Roswell Park Memorial Institute 1640 media (RPMI 1640; Welgene). Both cell lines were supplemented with 10% FBS (Welgene), penicillin and streptomycin (Welgene), and 4 mM L-glutamine (Welgene). The cells were subcultured using cell dissociation buffer (Gibco, Grand Island, NY, USA).

Mice
The MMTV-PyMT transgenic mice (FVB/NJ background) were obtained from Seok-Hyung Kim (Samsung Medical Center). C57BL/6 and Balb/c mice were purchased from DaehanBiolink (www.dhbiolink.com). All animals were maintained in the Laboratory of Molecular and Cellular Immunology Animal Facility at Inha University or in the facilities of Korea Bio in Korea University under the Use of Laboratory Animals guidelines and following proper protocols.

For genotyping of an MMTV-PyMT, the primer sequences used were 5′-GGAAGCAAGTACTTCACAAGGG-3′ and 5′-GGAAAGTCACTAGGAGCAGGG-3′.

For immunization, CFA/IFA (Sigma) or Imject Alum® (Thermo Fisher) was emulsified 1:1 (v/v) with 10 to 20 μg of Keyhole limpet hemocyanin (KLH) conjugated loop peptide (loop-KLH) or with scrambled sequence peptide as a control (9). The age matched MMTV-PyMT mice (4–6 wk) were immunized intraperitoneally for CFA or intramuscularly for alum 3 times within a 3-wk interval. The C57BL/6 mice and Balb/c mice were immunized with 5 μg of loop-KLH and CFA/IFA or alum 3 times within a 3-wk interval. Orthotopic breast cancer models and tumor size calculation methods have been previously described (9).

Eosinophil staining
Extracted tumor samples were immediately cut into 1 cm^3 pieces and immersed in 4% paraformaldehyde phosphate-buffered solution (WAKO, Osaka, Japan). After incubation overnight at 4°C, H&E stain protocol was performed by the Research Institute for Medical Sciences of Inha University.

ELISA
Blood sera were collected 3 days after the final injection and ELISA was performed as described previously (9). For isotyping, HRP-conjugated IgM, IgG1, IgG2a, IgG2c, and IgG3 (Southern Biotech, Birmingham, AL, USA) were used as secondary Abs.

Flow cytometric analysis
Small samples of mouse tumor tissues (2–3 wk after last immunization) were chopped in 1 ml of cell dissociation solution (1% 100 mg/ml collagenase/dispase, 0.5% 20 mg/ml DNase

in DMEM) and incubated for 30 min at 37°C. The cell suspension (1×10^5 to 1×10^6 cells) was stained for use in flow cytometry after blocking the Fc receptors by applying ultra-blocking buffer (10% normal mouse serum, 10% normal hamster serum, 10% normal rat serum, and monoclonal Ab 2.4G2 in PBS). Abs used were CD11c-FITC (eBioscience, San Diego, CA, USA), CD45-PE-Texas-Red (Invitrogen, Carlsbad, CA, USA), F4/80-PE-Cy5 (eBioscience), CD11b-biotin (Miltenyi, Bergisch Gladbach, Germany), Gr-1-PE-Cy7 (eBioscience), and SA-PerCP-Cy5.5 (eBioscience). All samples were filtered through a 200 μm nylon mesh before running in BD FACSAria. The results were analyzed by using the Flowjo 10 program (Tree Star, Inc., Ashland, OR, USA).

RNA sequencing

MMTV-PyMT mice were vaccinated 3 times in 3-wk intervals and were sacrificed 5 days after the final vaccination. The axillary and brachial lymph nodes were stored in RNAlater (Thermo Fisher, Waltham, MA, USA) and RNAs were extracted following the TRIzol (Invitrogen) protocol. The same quantities of RNA obtained from 3 mice were mixed to form one sample, and RNA sequencing was performed (Macrogen HiSeq4000; Illumina, Seoul, Korea). The abbreviated names of the various RNA sample groups are as following: WNI, FVB wild-type mice without any vaccination; WAL, wild-type mice vaccinated with loop metavaccine plus alum; WCL, wild-type mice vaccinated with loop metavaccine plus CFA; WAP, wild-type mice injected with alum; WCP, wild-type mice injected with CFA; MNI, PyMT mice without any immunization; MAL, PyMT mice injected with loop metavaccine plus alum; MCL, PyMT mice injected with loop metavaccine plus CFA; MAP, PyMT mice injected with alum without loop metavaccine; MCP, PyMT mice injected with CFA without loop metavaccine (**Supplementary Fig. 1**).

Bioinformatics analysis

From the initial 36,780 gene identities (ids) in the RNA expression profiles, those with 0 values in all samples, as well as pseudogenes, noncoding RNAs, and unidentified genes that do not have a specific name were eliminated from the list. The final pool included 24,953 different gene ids.

Differentially expressed gene (DEG) analysis, correlation matrix, hierarchical clustering, and heatmap analysis were performed using read counts and several R packages, including euclidean distance and complete linkage methods, in R version 3.5.3 (R Foundation, Vienna, Austria). DEG analysis was performed for 21 comparisons: WCP vs. WAP, WCL vs. WAL, MCP vs. MAP, MCL vs. MAL, WNI vs. WCP, MNI vs. MCP, WNI vs. WAP, MNI vs. MAP, WCP vs. WCL, WAP vs. WAL, MCP vs. MCL, MAP vs. MAL, WNI vs. WAL, WNI vs. WCL, MNI vs. MAL, MNI vs. MCL, WNI vs. MNI, WCP vs. MCP, WAP vs. MAP, WCL vs. MCL, and WAL vs. MAL. Among the comparisons, 11,517 different ids (6,504 unique genes) that were significantly different ($p < 0.05$) in at least one inter-group comparison were used for further analysis. The read counts were normalized following the z score calculation method prior to application in the heatmap analysis.

The 601 immune signature genes (**Supplementary Table 1**) for T cells, T_H cells, B cells, NKT cells, NK cells, monocytes, macrophages, neutrophils, and eosinophils were collected from PanglaoDB ([26]). The representative genes for immune cells were selected based on previous reports ([27]-[31]) and lists of commercially available specific Abs from Sino Biological and BioLegend. The eosinophil chemotaxis-related gene list was obtained from the Gene Ontology Browser of Mouse Genome Informatics (http://www.informatics.jax.org/).

Survival analyses of The Cancer Genome Atlas–human breast cancer (TCGA-BRCA) patients were performed using data obtained from the GDC Data Portal (https://portal.gdc.cancer.gov/). Patients with a known death date or with a known last-follow-up date of over 5 years were selected based on the available clinical data. The high and low expression levels and the median level of each gene were determined. The ER$^-$ patients were sorted based on estrogen receptor status included in the clinical data.

Statistical analysis
Statistical analyses were done by using GraphPad Prism 6 (GraphPad Software, San Diego, CA, USA). Unpaired 2-tailed t-test with equal SD was used in the statistical testing of group comparisons. Correlation analysis of *in vivo* assays was accomplished by using linear regression analysis programs. Survival graphs were analyzed by performing unpaired t-tests with Welch's correlation.

RESULTS

Polarized adjuvant effects on loop metavaccine efficacy in a PyMT mouse model
Our previous study showed that the KLH conjugated autoactivation loop of Prss14 was an effective immunogen resulting in the production of T_H1- and T_H2-type Abs and acting as an efficient preventive metastasis vaccine in 2 mouse models with tail-vein injection of syngeneic breast cancer cells (9). Hosts involved in the 2 mouse systems were the T_H1 dominant C57BL/6 strain and the T_H2 dominant Balb/c strain. Regardless of host type, the loop metavaccine functioned efficiently in reducing tumor progression and metastasis. To test metavaccine efficacy and determine the related mechanisms, we decided to test loop metavaccine with adjuvants in transgenic PyMT mice that produce breast cancer spontaneously.

We chose 2 widely used adjuvants, CFA and alum, with the hypothesis that they would produce different T_H responses. We measured the tumor sizes, metastasis status, and specific anti-loop Ab production after immunization. As expected from the previous study of tail-vein injection models (9), when CFA was used as an adjuvant, the loop metavaccine significantly reduced tumor growth and metastasis in PyMT mice compared to unimmunized mice or to immunized mice with a peptide containing scrambled sequence groups (**Fig. 1**). To our surprise, loop metavaccine with alum adjuvant, promoted tumor growth and metastasis (**Fig. 1A-D**). The results obtained with the alum adjuvant were unexpected because previous experiments in 2 tail-vein injected mouse models with the same alum adjuvant showed significantly beneficial metavaccine effects (9). In an attempt to explain this inconsistency, we hypothesized that it might be due to differences in the host's immune status that are induced by different adjuvant types in tumor-bearing mice.

The number of metastatic nodules in the mouse lungs are positively correlated with primary tumor weights (**Fig. 1E**), indicating that metastases and primary tumors were related events in both CFA and alum adjuvant situations. When the amount of total Abs was measured, the mice immunized with loop metavaccine and CFA (CFA-loop) established relatively more anti-loop specific Abs than mice immunized with loop metavaccine and alum (alum-loop) (**Fig. 1F**). In contrast, the levels of anti-loop Abs and both tumor and metastasis sizes showed negatively correlated relationships (**Fig. 1G**). These results suggest that the anti-tumor and anti-metastasis effects of the loop metavaccine may be mediated by the presence of specific Abs, but another factor may also be involved. It was surprising to find that Ab isotypes
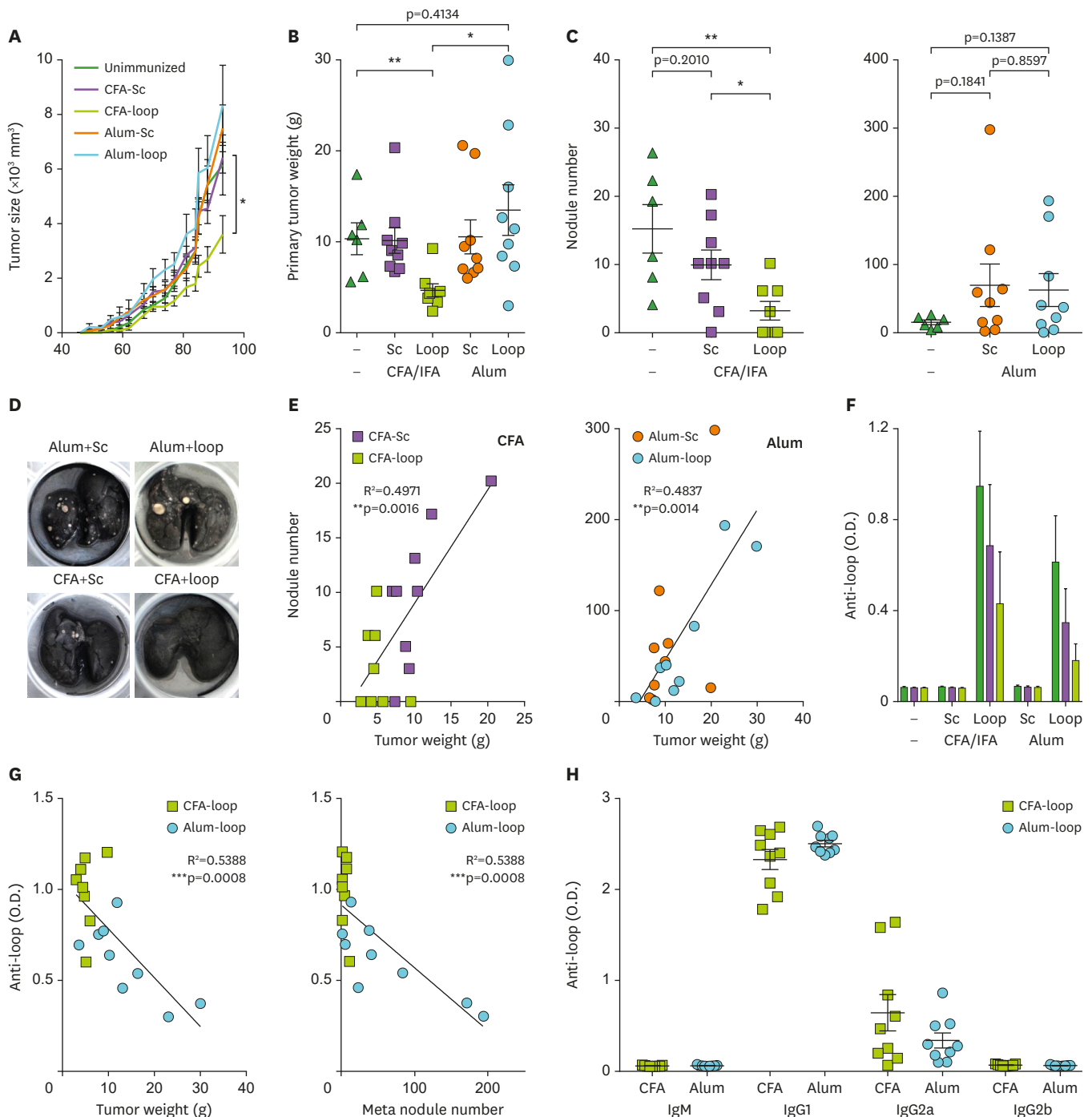
Figure 1. Polarizing influences of CFA or alum to loop metavaccination on tumor growth and lung metastasis in PyMT mice. (A) Average tumor growth curves were measured twice a week (n=5/group). Unimmunized vs. CFA-loop (*p=0.0115). (B) Primary tumor weights (*p=0.0110 and **p=0.0064). (C) Metastatic nodules. Left: CFA, right: alum (*p=0.0225 and **p = 0.0044). (D) Representative images of metastatic nodules. (E) Correlation analysis of primary tumor weights to metastatic nodules. (F) Anti-loop Ab production in PyMT mice tested by ELISA (green: 1:1,000, purple: 1:3,000, and yellow-green: 1:9,000 dilution). (G) Correlation analysis of the levels of anti-loop Ab with tumor weights (left) or metastatic nodule numbers (right). (H) Isotype analysis of the anti-loop Abs by ELISA.

immunized with loop metavaccine into PyMT mice induced both T_H1 and T_H2 types regardless of adjuvant types (**Fig. 1H**). It was previously shown that CFA induces T_H1 and T_H2 types while alum only induces T_H2 type (8,11).

These results indicate that a loop metavaccine can effectively reduce tumor growth and metastasis in PyMT mice, but only with the addition of an appropriate adjuvant such as CFA. However, loop metavaccine with alum adjuvant produced an unexpected adverse effect beyond the T_H paradigm by promoting tumor growth and metastasis in tumor-bearing PyMT mice.

Orthotopic breast cancer models also showed adjuvant-dependent contrasting loop metavaccine effects

To investigate whether the distinct effects of the CFA and alum adjuvants can be reproduced in other models, 4T1 and E0771 breast cancer cells were implanted orthotopically into their syngeneic hosts, Balb/c and C57BL/6 mice, respectively (**Fig. 2**). In the 4T1-Balb/c model, mice immunized with CFA-loop lived significantly longer than those immunized with alum-loop (**Fig. 2A**). Although primary tumor growth was not significantly different between the CFA-loop and alum-loop groups (**Fig. 2B**), metastasis was reduced in the CFA-loop group (**Fig. 2C**). In the alum-loop group, 2 out of 5 animals showed a greater amount of metastasis in the lungs but the average lung weight was not significantly different from those in the CFA-loop group (**Fig. 2C**). In addition, the numbers of metastatic nodules were inversely correlated with that of anti-loop specific Abs (**Fig. 2D**), suggesting that the presence of anti-loop Abs was
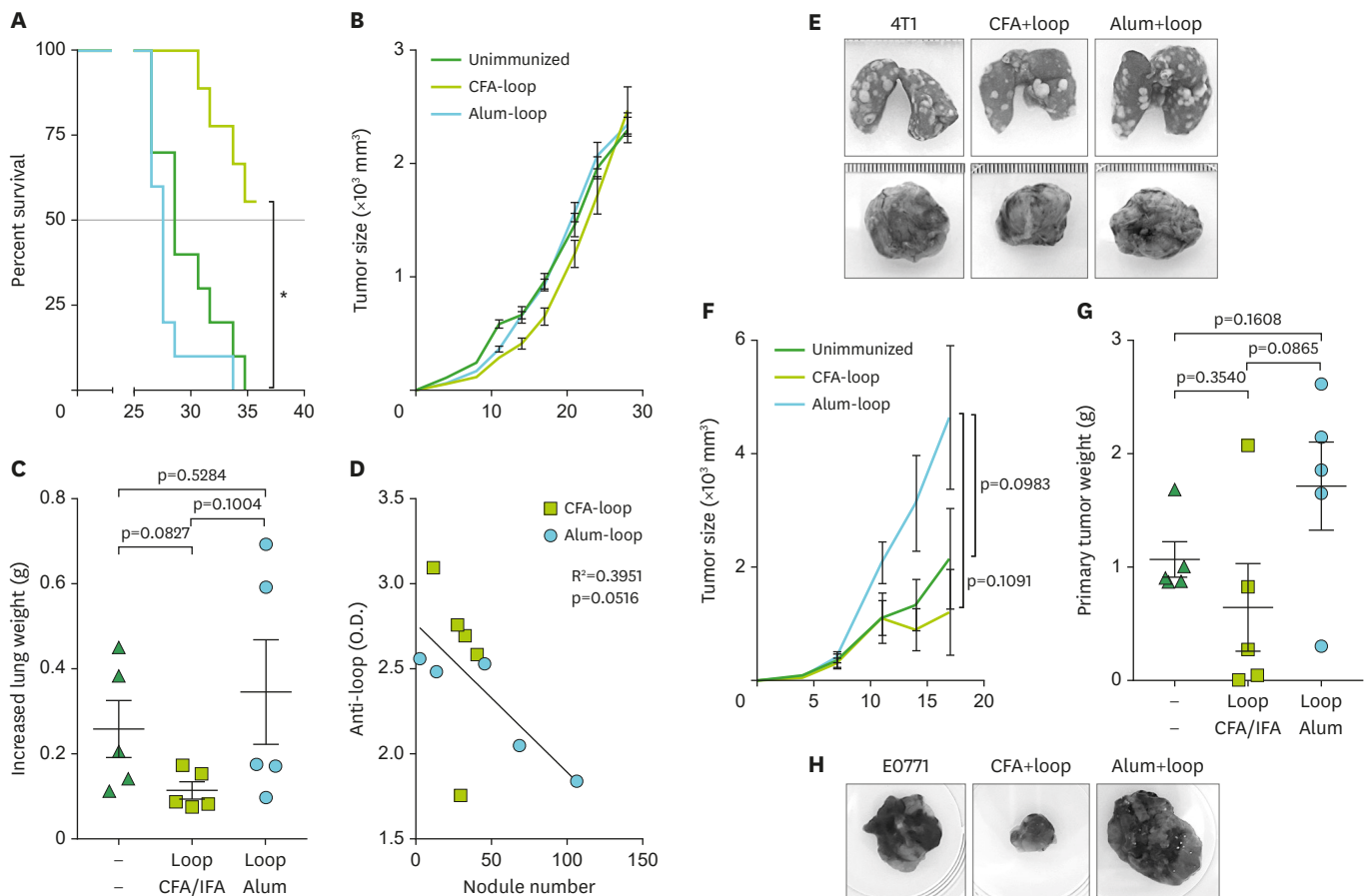
Figure 2. Bipolarizing adjuvant effects of CFA and alum on loop metavaccine in 4T1- and E0771-orthotopic transplantation models. (A-E) 4T1-Balb/c orthotopic system. (A) Survival curve of 4T1 orthotopic mouse with immunization (n=10 per group) (*p=0.0445). Unimmunized: green line, CFA-loop: yellow green line, alum-loop: blue line. Post-transplantation days are indicated on the X-axis. (B) Average of tumor growth curves (n=5). (C) Lung weights on the day of sacrifice. The average value of non-tumor-bearing lungs (n=5) was subtracted. (D) Correlation analysis of anti-loop Abs to the numbers of metastatic nodules. (E) Representative images of 4T1 metastatic nodules on lungs. (F-H) E0771-C57BL/6 orthotopic system. (F) Average of tumor growth curves (n=10). (G) Primary E0771 tumor weights on the day of sacrifice. (H) Representative images of E0771 primary tumor on the day of sacrifice.

involved in reducing the amount of metastasis. Similarly, in the E0771-C57BL/6 orthotopic mouse model, primary tumor growth slightly decreased following immunization with the CFA-loop but increased with the alum-loop injection (**Fig. 2F-H**). The number of E0771 metastatic nodules in the host was not countable at the time of examination, probably due to the low metastatic nature of the E0771 cell line. However, overall results support the notion that the effects of loop metavaccine are influenced by the type of adjuvant.

When Ab isotypes were examined, the 2 tumor-bearing hosts in orthotopic models revealed the presence of both T_H1 and T_H2 Ab isotypes when immunized with loop metavaccine regardless of adjuvant type (**Supplementary Fig. 2B and D**). In the case of wild-type mice without tumor implantation, treatment with CFA-loop revealed T_H1 and T_H2 type Ab responses while alum-loop only revealed T_H2 type Ab response in normal C57BL/6 mice (**Supplementary Fig. 2E**). Therefore, we concluded that the presence of both T_H1 and T_H2 type Abs following loop metavaccine immunization is the feature of tumor-bearing mice regardless of adjuvant type.

Tumor-infiltrating myeloid cells play roles in the polarizing effects of adjuvants with loop metavaccine

To identify the types of immune cells involved in the polarizing effects of adjuvants on loop metavaccine efficacy, CD45+ immune cells in PyMT tumor tissues were analyzed by flow cytometry. While we failed to detect any significant differences between CFA-loop and alum-loop groups in the population of lymphoid cells, we observed that the myeloid cell population showed interesting differences. Especially the CD11b+F4/80+Gr1-SSC^{high} cells, which are likely eosinophils ([32]), were significantly different (**Fig. 3B**). The tumor tissues of mice immunized with CFA-loop contained higher population levels of CD11b+F4/80+Gr1-SSC^{high} cells (**Fig. 3B**) and relatively lower CD45+ percentages than to unimmunized or alum-loop tumor tissues (**Fig. 3B**). In addition, the numbers of eosinophil-type cells of loop injected mice were significantly inversely correlated to the degree of primary tumor progression and metastasis (**Fig. 3C**). On the other hand, the numbers of eosinophil-type cells were positively correlated to the levels of anti-loop Abs in a statistically significant fashion (**Fig. 3D**). These results suggest that the eosinophil population in tumor tissues can take part in the effects of the loop metavaccine.

In the orthotopic E0771 tumor tissues, the frequencies of CD11b+Siglec-F+ eosinophil were higher in CFA-loop vaccinated mice than in the tumors from alum-loop vaccinated mice but in a less significant fashion (**Fig. 3F**). In the E0771 tumors, a negative correlation between eosinophil population level and tumor weight was distinct (**Fig. 3G**).

In order to verify the presence of eosinophils in the PyMT tumor tissues, immunohistochemistry analysis was undertaken (**Fig. 4**). The number of eosinophils in tumor tissues was clearly higher in CFA-loop mice than in alum-loop mice with statistical significance (**Fig. 4B**). It is clear that the increase of eosinophil number was loop metavaccine dependent. These results suggest that eosinophil can be an important parameter in polarizing adjuvant effects on loop metavaccine efficacy.

Other myeloid cell-type populations were also significantly different between the 2 adjuvant types. The CD11b+F4/80+Gr1^{int} cell population, a representative monocyte type, had a higher fraction of tumor tissues of CFA-loop vaccinated mice than in unimmunized PyMT mice (**Fig. 5A**). The fraction of those cells in alum-loop vaccinated mice was lower than those in CFA-loop vaccinated mice, but the difference was not statistically significant. The
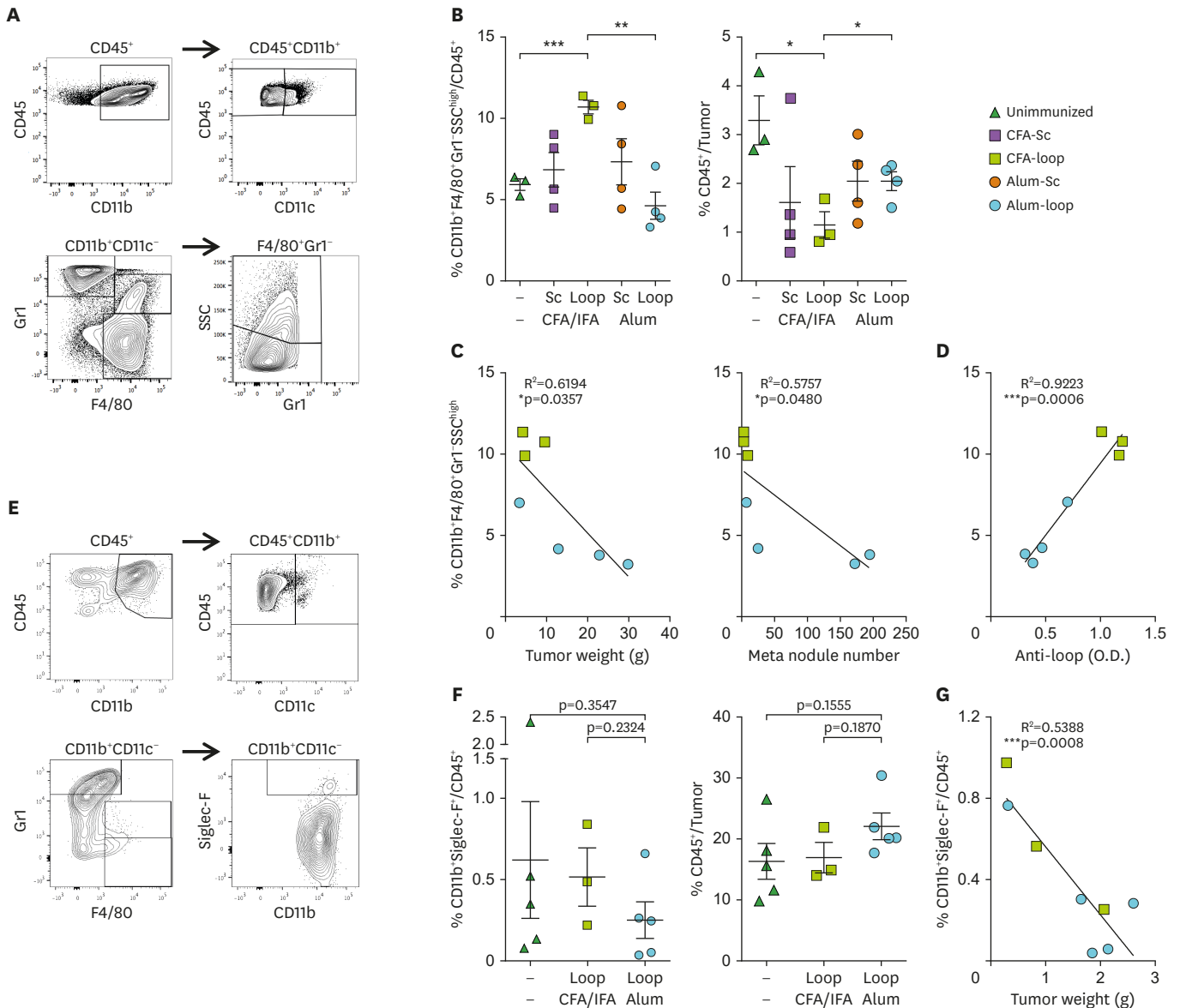
Figure 3. Analysis of infiltrating myeloid cells in PyMT and E0771 tumor tissues. (A-D) Analysis of tumor-infiltrating cells in PyMT mice. (A) Gating with markers of PyMT tumor-infiltrating myeloid cell profiles. (B) Tumor CD11b$^+$F4/80$^+$Gr1$^-$SSC^{high} frequencies in CD45$^+$ cells (left) (**p=0.0022 and ***p=0.0010). CD45$^+$ lymphoid cell frequencies in total live tumor cell (right). Unimmunized vs. CFA-loop (*p=0.0197) and CFA-loop vs. alum-loop (*p=0.0385), respectively. (C) Correlation analysis of tumor-infiltrating eosinophil frequencies to tumor weight (left) or to the number of metastatic nodules on lung (right). (D) Correlation analysis of the levels of anti-loop Ab with tumor eosinophil frequencies. (E-G) Analysis of tumor-infiltrating cells of E0771-C57BL/6 orthotopic mice. (E) Gating with markers of E0771 tumor-infiltrating myeloid cell profiles. (F) CD11b$^+$Siglec-F$^+$ eosinophil frequencies in CD45$^+$ cells (left). CD45$^+$ lymphoid frequencies in total live tumor cell (right). (G) Correlation analysis of the CD11b$^+$Siglec-F$^+$ eosinophil frequencies to primary tumor weights.

percentage of CD11b$^+$F4/80$^+$Gr1^{int} monocytes was inversely correlated to tumor weight with statistical significance, but, not to the metastasis (**Fig. 5B**). Interestingly the percentage of CD11b$^+$F4/80$^+$Gr1^{int} monocytes was directly correlated to the amount of anti-loop Abs (**Fig. 5C**).

In contrast, CD11b$^+$F4/80$^-$Gr1^{high} cells, presumably neutrophils, showed higher fractions of tumor tissues in alum-loop vaccinated mice than in CFA-loop vaccinated mice (**Fig. 5D**), and the percentage of CD11b$^+$F4/80$^-$Gr1^{high} neutrophils was linearly correlated to tumor weight, but not to the degree of metastasis (**Fig. 5E**). The percentage of CD11b$^+$F4/80$^-$Gr1^{high}
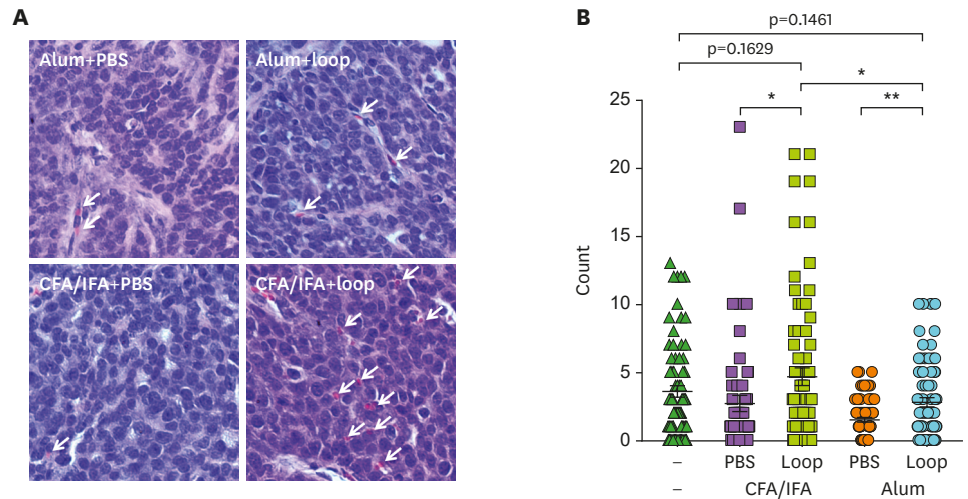
Figure 4. Eosinophils in H&E stained PyMT tumor sections. (A) Immunization methods are indicated on top of the pictures. The white arrows indicate eosinophils. (B) Quantification of eosinophil counts. Eosinophils were counted from 18 areas per sample. Unimmunized (n=4), CFA-PBS (n=3), CFA-loop (n=4), alum-PBS (n=4), and alum-loop (n=4). CFA-PBS vs. CFA-loop (*p=0.0325), alum-PBS vs. alum-loop (**p=0.0010), and CFA-loop vs. alum-loop (*p=0.0116), respectively.

neutrophils was inversely correlated to the amount of loop Abs (**Fig. 5F**). These data suggest that neutrophil population induced by alum may have adversely influenced the outcome of loop vaccination.

Adjuvants of loop metavaccine can modify PyMT host immune parameters

To systemically analyze factors involved in immune cells and their function in tumor-bearing mice, we undertook bioinformatics-based analyses that used RNA sequencing of samples from the lymph nodes of normal and PyMT mice after immunization with various combinations of CFA, alum, and loop metavaccine (**Supplementary Fig. 1**). This scheme involved a total of 10 different combinations of immunizations (CFA or alum with or without loop metavaccine) with normal FVB mice and tumor-bearing PyMT mice. We chose a time point that is earlier than the end point of tumor progression and metastasis. The overall expression comparison of the gene collection from a total of 21 DEGs within the correlation matrix showed clustering of expression profiles (**Fig. 6A**). Overall comparisons of each group revealed approximately 70% similarity of groups, except for WCL that had an approximation of 50% similarity to the other groups. Interestingly, loop metavaccine-associated group (WAL, WCL, MAL, and MCL) genes were distant from the unimmunized group genes (WNI, WAP, WCP, MNI, MAP, and MCP) regardless of the adjuvant type used (**Fig. 6A**). Based on these results, we concluded that loop metavaccine, not adjuvant types, produced greater changes in whole-host expression profiles.

When the 601 immune signature genes (**Supplementary Table 1**) were compared, the matrix revealed that the wild type FVB groups (from WAL to WNI) and PyMT groups (from MAL to MNI) were clustered separately (**Fig. 6B**). Among these, the MCP to WCP showed 96% similarity and the MCL to WCL showed 89% similarity, suggesting that loop vaccination induces differential immune signature gene expressions rather than from the presence of the tumor itself. However, MAP to WAP and MAL to WAL groups had only 79% and 76% similarities, respectively, suggesting that the alum adjuvant can markedly modify immune signature expressions. Results of hierarchical clustering in pedigree types showed that
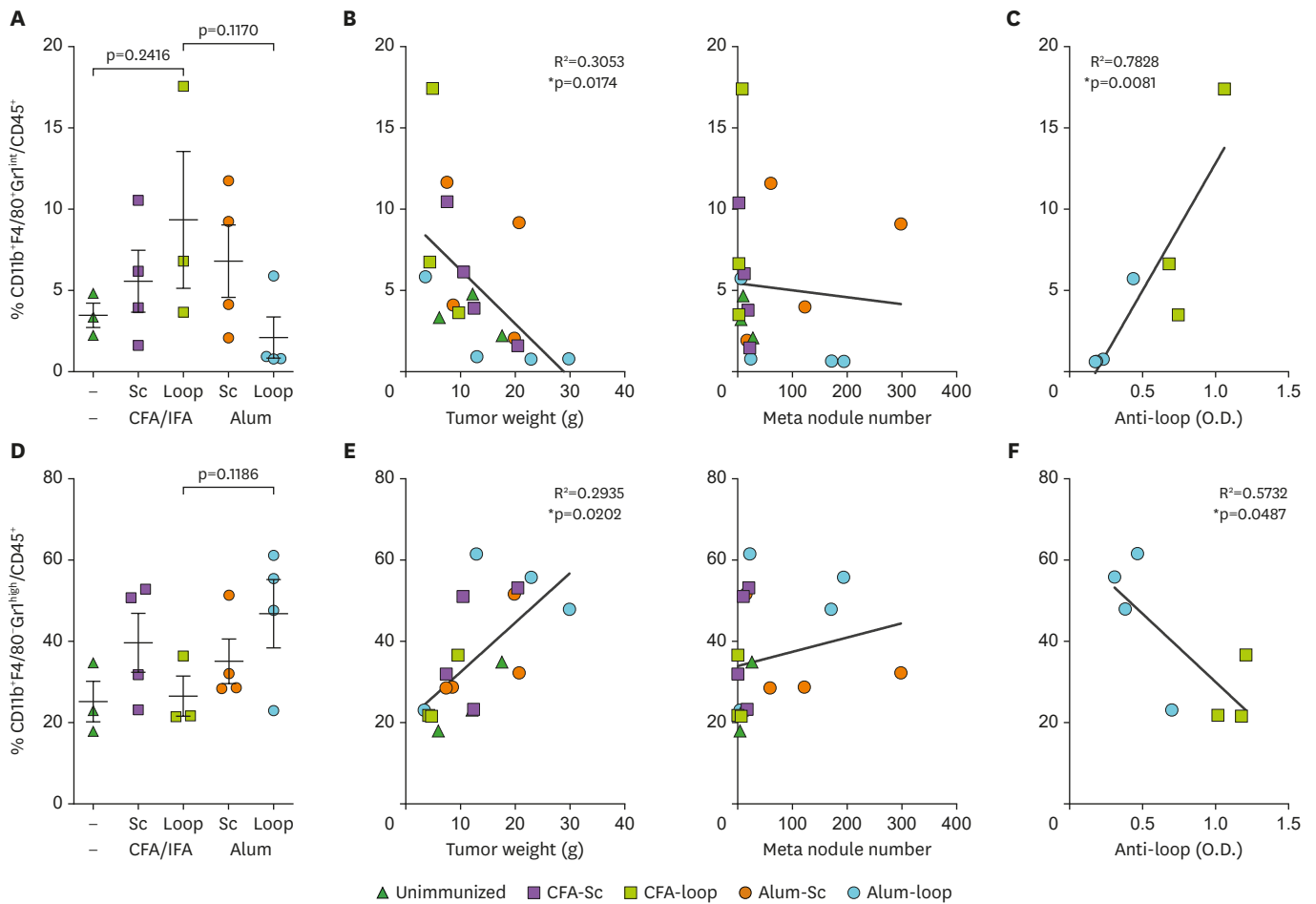
Figure 5. Analysis of infiltrating monocytes and neutrophils in PyMT tumors. (A) Tumor CD11b$^+$F4/80$^+$Gr1^{int} monocyte frequencies in CD45$^+$ cells. (B) Correlation analysis of monocyte frequencies to the primary tumor weights (left) or to the number of metastatic nodules on lungs (right). (C) Correlation analysis of the levels of anti-loop Ab to the monocyte frequencies. (D) Tumor CD11b$^+$F4/80$^-$Gr1^{high} neutrophil frequencies in CD45$^+$. (E) Correlation analysis of neutrophil frequencies to the tumor weight (left) and to the numbers of metastatic nodules on lungs (right). (F) Correlation analysis of the levels of anti-loop Ab to the neutrophil frequencies.

MCL and MAL were the most distant groups. MCL was isolated from other clusters, while MAL was close to MNI (**Fig. 6B**). These results suggest that CFA can uniquely influence loop metavaccine effects by modifying the host's immune system when a tumor is present.

Systemic changes in lymphoid and myeloid cell-specific gene expressions depend on the host and the immunization protocol

To examine the immune cell types, we selected cell type specific immune signature genes and analyzed them by clustering their expression patterns (**Fig. 7**). The heatmap of the lymphoid cell type specific genes showed clear patterns with separate clustering of PyMT and wild-type groups (**Fig. 7A**). The representative signatures of B cell, pan T cell signature genes were expressed at higher levels in wild-type lymph nodes (from WNI to WCL) than in PyMT lymph nodes (from MNI to MCL). To investigate the T$_H$ paradigm, we chose T$_H$ subset-specific transcription factors and representative effector cytokines: T-bet and IFN-γ for T$_H$1, Gata3 and IL-4 for T$_H$2, RORγt and IL-17 for T$_H$17, Bcl-6 and IL-21 for T$_{FH}$, and Foxp3 and TGF-β for T$_{reg}$ (30). In loop vaccinated PyMT lymph nodes (MAL and MCL), the expressions of the T$_H$1 and T$_{reg}$ signature genes were lower, and the expressions of T$_H$2 and T$_H$17 signature genes were

IMMUNE
NETWORK
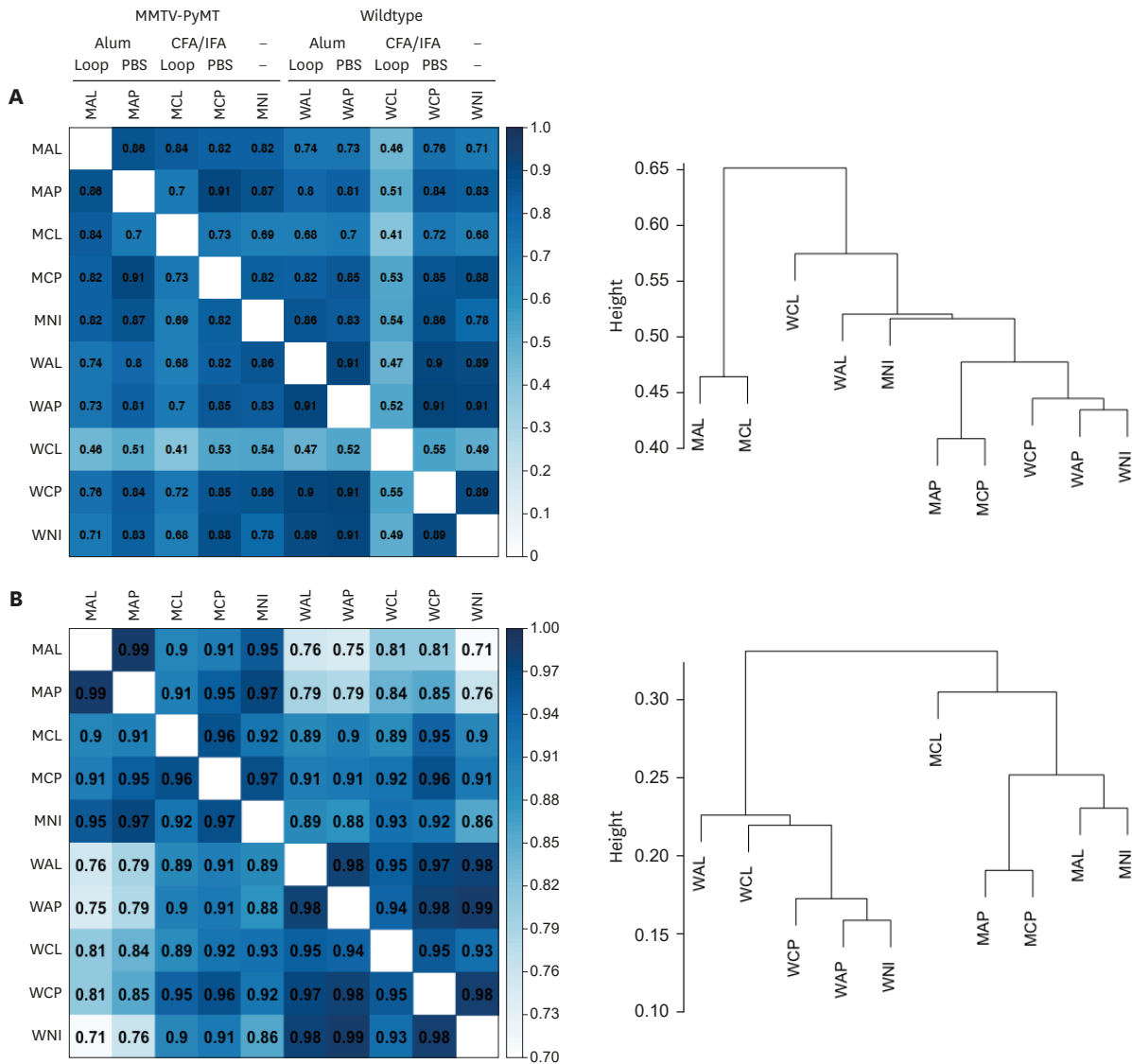
Figure 6. Similarity analyses of RNAseq with correlation matrices and hierarchical clusters. (A) Correlation matrix comparing the overall gene expression profiles (left), and hierarchical clustering showing the distances among the groups (right). Bar: 0 (white) to 1 (dark blue). (B) Correlation matrix comparing the overall immune profiles (left), and hierarchical clustering showing the distances among the groups (right). The names of each group are mentioned in the materials and methods. Bar: 0.7 (white) to 1.0 (black).

higher than those of other lymph nodes (**Fig. 7A**). Furthermore, the St14 gene (Prss14) and the Spint1 and Spint2 genes (2 inhibitors of Prss14) were also highly expressed in the MAL and MCL lymph nodes. These results suggest that loop vaccination in the PyMT model directly modifies both the T_H paradigm and Prss14 expression in lymphoid cells (**Fig. 7A**). In contrast, second signal signatures that are important in immune costimulatory and inhibitory checkpoints showed no clear clustering patterns (**Supplementary Fig. 3**) with all lymph node samples, suggesting that those genes are not critically involved in the loop metavaccine immunization protocol of this study.

Next, we analyzed myeloid cell signatures. Loop vaccination with the 2 adjuvant types (MCP vs. MCL and MAP vs. MAL) showed different expression patterns in almost all the myeloid cell type genes analyzed (**Fig. 7B**). Interestingly, eosinophil marker genes were much higher

Figure 7. Expression profile analyses of signature genes specific to immune cells and eosinophil chemoattractants. (A) Heatmap of selected signature genes and transcription factors for lymphoid cells along with Prss14 (St14) and its inhibitors (Spint1 and Spint2). (B) Heatmap of selected signature genes for myeloid cells. (C) Heatmap analysis of selected eosinophil chemoattractants (top). Hierarchical clustering of eosinophil chemoattractant gene profiles (bottom). Color key: −2.0 (green) to 2.0 (red). Group names are at the bottom.

in the alum-loop treated lymph nodes (MAP and MAL) than in CFA-loop treated lymph nodes (MCP and MCL). Alum-loop vaccination (MAL) produced the highest expressions among the eosinophil markers. This result initially appeared to contradict the observation that CFA-loop produced more eosinophils in PyMT tumor tissues analyzed by flow cytometry (**Figs. 3** and **4**).

To elucidate this apparent contradiction, we checked whether eosinophil chemotaxis is part of the explanation since the immune signatures were taken from lymph nodes instead of tumor tissues (**Fig. 7C**). The gene expression levels related to eosinophil chemotaxis were divided into 2 clusters, wild-type (from WNI to WCL) and PyMT (from MNI to MCL). Among the PyMT groups, loop vaccinated with adjuvants (MAL and MCL) had high expressions of Ccl6 and Ccl9, which are Ccr1 ligands (**Fig. 7C** top), suggesting that these genes depend more on the presence of loop metavaccine than on the type of adjuvant used. On the other

hand, Ccl1, Ccl4, Ccl7, and Cx3Cl1 were notably high in MCL while Ccr3, Ccl24, and Ccl8 were high in MAL (**Fig. 7C**). The observed hierarchical clustering of eosinophil chemotaxis-related genes supports the observed difference between MCL and MAL (**Fig. 7C**). Therefore, we concluded that eosinophil chemotaxis could be involved in the distinct adjuvant influence differences between CFA-loop and alum-loop.

Eosinophil chemotactic genes influence the survival of high ST14 patients

To investigate the significance of eosinophils in the survival of human breast cancer patients, we examined the survival data of human breast cancer patients from TCGA and the patients' profiles of the eosinophil marker gene SIGLEC-8 and the eosinophil chemotactic genes, CCL4, eotaxin-1 (CCL11), eotaxin-2 (CCL24), and eotaxin-3 (CCL26) (**Fig. 8**). Patients with high expressions of SIGLEC-8, CCL24, and CCL4 had significantly higher survival rates (**Fig. 8A**). As the ST14^{high} patients reported to have poor survival (21), we examined the gene expressions within the ST14^{high} patients. Among the ST14^{high} patients, when the eosinophil gene expression level was high, especially CCL4 and CCL24, the patients lived significantly longer (**Fig. 8B**). Furthermore, since the survival rates of ST14^{high} and ER[-] patients are very poor (21), we examined the survival within ST14^{high}ER[-] patients and observed that the survival of CCL4^{low}ST14^{high}ER[-] patients was markedly lower (**Fig. 8C**). These results indicate that high expression of eosinophil marker SIGLEC-8 or chemokines CCL4 and CCL24 can result in the improved survival of breast cancer patients with a high expression of ST14. Thus, we conclude that eosinophil chemotaxis can improve the survival of ST14^{high} patients.

DISCUSSION

In this report, we show that the use of different adjuvants can critically influence the host's immune response when the adjuvants are applied with loop metavaccine. In 3 tumor-bearing animal models, the use of CFA enhanced loop metavaccine's effect, while the use of alum adversely affected vaccination outcomes. Immune parameter analyses suggested that myeloid components, especially eosinophils, have an important part in this paradigm.

In our previous report, we attempted to set up for the preventive metastasis vaccine that is applicable to post-surgery cancer patients. The loop metavaccine applied through tail-vein injection was shown to effectively reduce cancer metastasis when either CFA or alum was used as adjuvants (9). However, we realized that preventive immunization protocol to naïve animals without tumor and challenging tumor cells later is not the correct post-surgery model. In addition, we could not find literature on the patient immune profiles and there are too many unknowns in the host immune status. Therefore, we decided to use tumor-bearing mouse models such as PyMT and 2 orthotopic models. The loop metavaccine surprisingly produced contradictory results from the 2 adjuvant types assessed. The CFA with loop metavaccine effectively reduced cancer progression and metastasis while the alum with loop metavaccine promoted cancer growth and metastasis (**Figs. 1** and **2**).

These unexpected results were not due to a T_H paradigm shift as we initially suspected. As shown in **Supplementary Fig. 2B and D**, tumor-bearing animals showed both T_H1- and T_H2-type anti-loop Abs regardless of whether the host's dominant immune response was T_H1 (C57BL/6) or T_H2 (Balb/c). This is in contrast to the results obtained from non-tumor-bearing loop metavaccine immunized mice (**Supplementary Fig. 3E**). Regardless, the levels of anti-loop Abs of any isotype were well correlated to the reduction of tumor size and metastasis
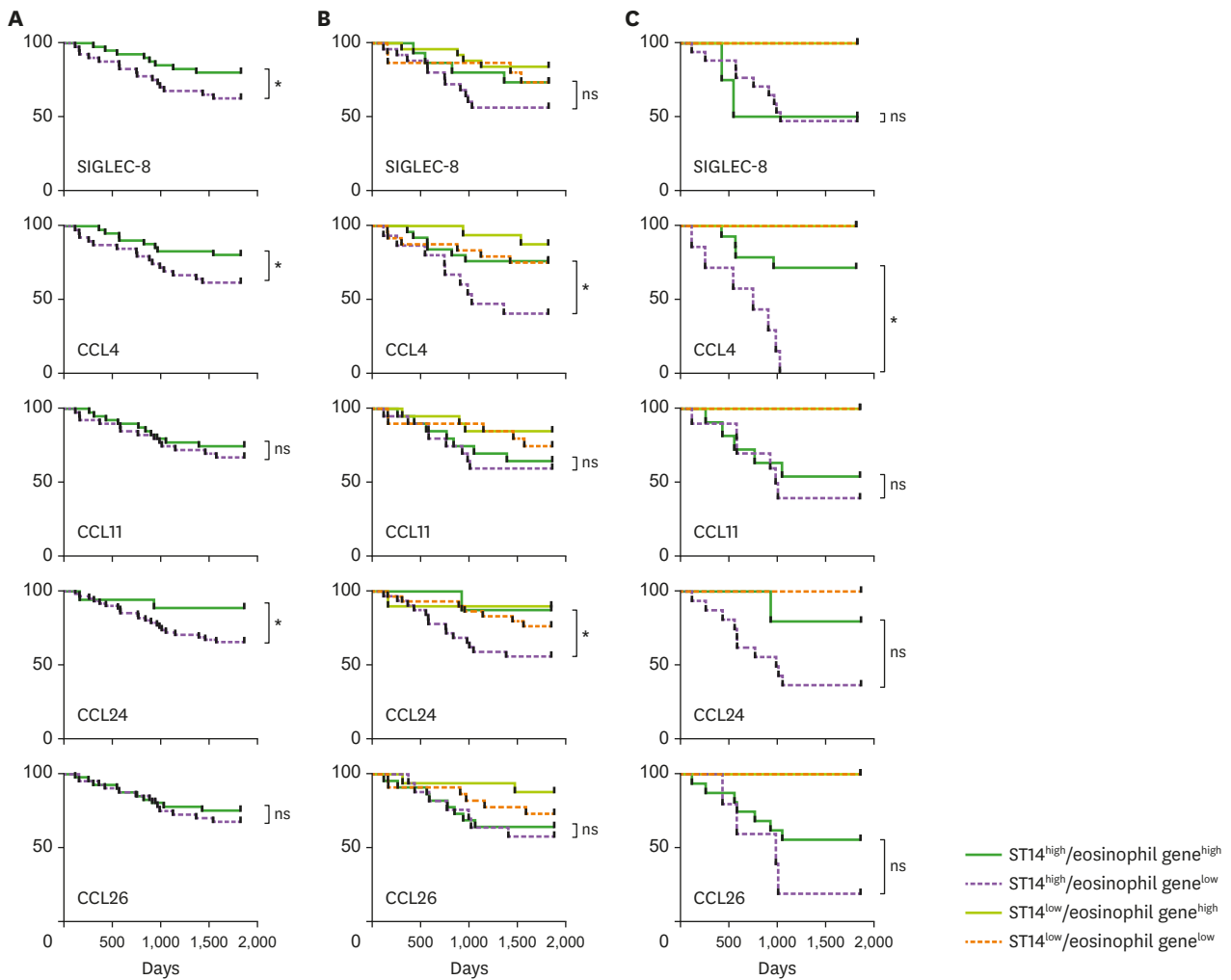
Figure 8. Survival plots of TCGA-BRCA patients with eosinophil signatures and ST14 expression. SIGLEC-8, CCL4, CCL11, CCL24, and CCL26 RNA expression profiles of breast cancer patients (n=80) were collected from TCGA. (A) Survival curve of total breast cancer patients by eosinophil gene expression levels (high expression: green solid line, low expression: purple dotted line). SIGLEC8^{high} vs. SIGLEC8^{low} (*p=0.0270), CCL4^{high} vs. CCL4^{low} (*p=0.0178), and CCL24^{high} vs. CCL24^{low} (*p=0.0146). (B) Survivals of patients with eosinophil gene expression in ST14^{high} patients. ST14^{high}CCL4^{high} vs. ST14^{high}CCL4^{low} (*p=0.0172), ST14^{high}CCL24^{high} vs. ST14^{high}CCL24^{low} (*p=0.0372). (C) Survival of ER⁻ patients with eosinophil gene expression amongST14^{high} patients (n=27). ER⁻ST14^{high}CCL4^{high} vs. ER⁻ST14^{high}CCL4^{low} (*p=0.0332). ns, not significant.

(**Figs. 1G** and **2D**). Therefore, it suggests that the levels of specific Abs, not isotypes, are important for loop vaccine efficacy.

The immune signatures of tumor bearing mice are very different from normal mice regardless of immunization protocol (**Figs. 6** and **7**). Overall differences between normal and cancer bearing mice were clearly visible in both matrix type and pedigree type analyses regardless of immunization protocols. This difference may be the main cause of unexpected experimental results from our previous study to this study.

In an effort to identify important host immune parameters related to adjuvant type that influence loop vaccine efficacy, we took 2 approaches, the examination of flow cytometry of tumor-infiltrating immune cells at the late stage of tumor with metastasis and the systemic profiling of immune signature genes of lymph nodes using a combinatorial immunization protocol at the earlier stage of tumor without detectable metastasis. The flow cytometric analysis
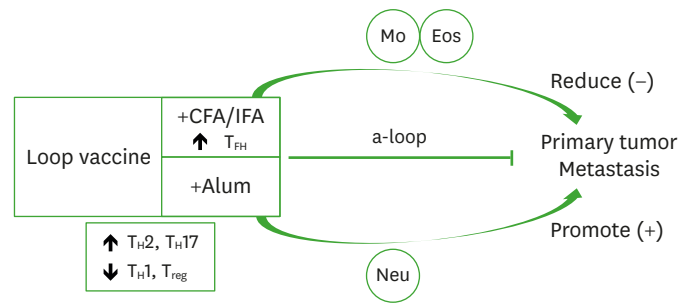
Figure 9. Model of immunological influences involved in the effects of loop metavaccine immunization against breast cancer.

of tumor-infiltrating immune cells revealed that eosinophil and monocyte levels were highly related to CFA-loop metavaccine efficacy, while neutrophils appeared to have an adverse role in the cancer-promoting effect of the alum-loop metavaccine (**Figs. 3-5**). Although the effects of monocytes and neutrophils following loop vaccination have not been fully described, it appears that the myeloid component can critically affect vaccine efficacy. The results in **Fig. 7B** support this suggestion as it shows that myeloid patterns are modified by loop vaccination. However, results for the immune cell signature genes provided limited support to the suggestion that monocytes and neutrophils are involved. The eosinophil chemoattractant profiling revealed distinct differences between the 2 adjuvants (**Fig. 7C**). In addition, different types of eosinophil chemoattractants were involved in the contrasting effects of CFA-loop and alum-loop. Ccl4 was expressed at a higher level in CFA-loop (**Fig. 7C**) than in alum-loop vaccinations. This can be explained by the fact that Ccl4 is involved in extravasation and migration of eosinophils and monocytes (33). Survival analysis results for the assessment of CCL4 gene expression in $ST14^{high}$ patients (**Fig. 8B and C**) supported the notion that CCL4 could be the key chemoattractant for anti-cancer eosinophils involved in the loop metavaccine effect.

It is interesting that loop metavaccine, regardless of adjuvant types, can change the T_H response (**Fig. 7A**). It remains unclear how T_H subtypes are involved in the loop metavaccine effects; however, T_H2-dependent eosinophil prevalence may come from a T_H2 shift induced by loop vaccination (34). In addition, the increased T_{FH} signatures of MCL can help produce higher amounts of specific anti-loop Abs in CFA-loop vaccinated mice (**Figs. 1F** and **7A**).

Finally, we summarized the results to form a simple model of loop metavaccine effects by adjuvant types (**Fig. 9**). In this model, the loop metavaccine predominantly increases T_H2 and T_H17 immune responses and decreases T_H1 and T_{reg} responses without being affected by the type of adjuvant. The CFA-loop vaccine generates more specific Ab responses; beneficial eosinophil and monocyte responses to reduce tumor growth and metastasis. On the other hand, the alum-loop vaccine produces neutrophil responses, promoting tumor growth and metastasis. Consequentially, loop vaccine with CFA leads immune editing to beneficial effects on tumors and metastases, whereas that with alum leads to adverse effects on tumors and metastases.

ACKNOWLEDGEMENTS

IMMUNE NETWORK

SUPPLEMENTARY MATERIALS

Supplementary Table 1
Immune signature gene lists

Click here to view

Supplementary Figure 1
Groups with various immunization protocols and control. Group names were determined based on the host, adjuvant types, and the presence of antigen.

Click here to view

Supplementary Figure 2
Ab isotype analyses on the loop vaccine with CFA or with alum. (A) Levels of anti-loop Abs form tumor-bearing Balb/c mice immunized with loop metavaccine tested by ELISA. (B) Isotypes of anti-loop Ab in orthotopic 4T1-Balb/c immunized with loop metavaccine. Left: CFA, right: alum. (C) Levels of anti-loop Abs in orthotopic E0771-C57BL/6 immunized with loop metavaccine tested by ELISA. (D) Isotypes of anti-loop Ab in orthotopic E0771-C57BL/6 immunized with loop metavaccine. Left: CFA, right: alum. (E) Analysis of anti-loop Ab isotypes in wild type C57BL/6 mice. The 2 µg of loop-KLH peptide emulsified 1:1 with CFA or with alum or with MF59 or with CpG-IDNs. The detected T_H types are written in the graph.

Click here to view

Supplementary Figure 3
Gene profile analyses of immune checkpoints in draining lymph nodes. (A) Heatmap analysis of co-stimulatory immune checkpoint genes. (B) Heatmap analysis of inhibitory immune checkpoint genes. Color key: −2.0 (green) to 2.0 (red).

Click here to view

REFERENCES

1. Hanahan D, Weinberg RA. Hallmarks of cancer: the next generation. *Cell* 2011;144:646-674.
   PUBMED | **CROSSREF**
2. Schreiber RD, Old LJ, Smyth MJ. Cancer immunoediting: integrating immunity's roles in cancer suppression and promotion. *Science* 2011;331:1565-1570.
   PUBMED | **CROSSREF**
3. Lewis CE, Pollard JW. Distinct role of macrophages in different tumor microenvironments. *Cancer Res* 2006;66:605-612.
   PUBMED | **CROSSREF**
4. Sionov RV, Fridlender ZG, Granot Z. The multifaceted roles neutrophils play in the tumor microenvironment. *Cancer Microenviron* 2015;8:125-158.
   PUBMED | **CROSSREF**
5. Kim HJ, Cantor H. CD4 T-cell subsets and tumor immunity: the helpful and the not-so-helpful. *Cancer Immunol Res* 2014;2:91-98.
   PUBMED | **CROSSREF**
6. Chraa D, Naim A, Olive D, Badou A. T lymphocyte subsets in cancer immunity: friends or foes. *J Leukoc Biol* 2019;105:243-255.
   PUBMED | **CROSSREF**

7. Ise W, Fujii K, Shiroguchi K, Ito A, Kometani K, Takeda K, Kawakami E, Yamashita K, Suzuki K, Okada T, et al. T follicular helper cell-germinal center B cell interaction strength regulates entry into plasma cell or recycling germinal center cell fate. *Immunity* 2018;48:702-715.e4.
   PUBMED | CROSSREF

8. Billiau A, Matthys P. Modes of action of Freund's adjuvants in experimental models of autoimmune diseases. *J Leukoc Biol* 2001;70:849-860.
   PUBMED

9. Kim KY, Yoon M, Cho Y, Lee KH, Park S, Lee SR, Choi SY, Lee D, Yang C, Cho EH, et al. Targeting metastatic breast cancer with peptide epitopes derived from autocatalytic loop of Prss14/ST14 membrane serine protease and with monoclonal antibodies. *J Exp Clin Cancer Res* 2019;38:363.
   PUBMED | CROSSREF

10. Di Pasquale A, Preiss S, Tavares Da Silva F, Garçon N. Vaccine adjuvants: from 1920 to 2015 and beyond. *Vaccines (Basel)* 2015;3:320-343.
    PUBMED | CROSSREF

11. Marrack P, McKee AS, Munks MW. Towards an understanding of the adjuvant action of aluminium. *Nat Rev Immunol* 2009;9:287-293.
    PUBMED | CROSSREF

12. Tomljenovic L, Shaw CA. Aluminum vaccine adjuvants: are they safe? *Curr Med Chem* 2011;18:2630-2637.
    PUBMED | CROSSREF

13. Darbre PD, Mannello F, Exley C. Aluminium and breast cancer: sources of exposure, tissue measurements and mechanisms of toxicological actions on breast biology. *J Inorg Biochem* 2013;128:257-261.
    PUBMED | CROSSREF

14. Kim MG, Chen C, Lyu MS, Cho EG, Park D, Kozak C, Schwartz RH. Cloning and chromosomal mapping of a gene isolated from thymic stromal cells encoding a new mouse type II membrane serine protease, epithin, containing four LDL receptor modules and two CUB domains. *Immunogenetics* 1999;49:420-428.
    PUBMED | CROSSREF

15. Lin CY, Anders J, Johnson M, Sang QA, Dickson RB. Molecular cloning of cDNA for matriptase, a matrix-degrading serine protease with trypsin-like activity. *J Biol Chem* 1999;274:18231-18236.
    PUBMED | CROSSREF

16. Takeuchi T, Shuman MA, Craik CS. Reverse biochemistry: use of macromolecular protease inhibitors to dissect complex biological processes and identify a membrane-type serine protease in epithelial cancer and normal tissue. *Proc Natl Acad Sci U S A* 1999;96:11054-11061.
    PUBMED | CROSSREF

17. Benaud CM, Oberst M, Dickson RB, Lin CY. Deregulated activation of matriptase in breast cancer cells. *Clin Exp Metastasis* 2002;19:639-649.
    PUBMED | CROSSREF

18. Bergum C, Zoratti G, Boerner J, List K. Strong expression association between matriptase and its substrate prostasin in breast cancer. *J Cell Physiol* 2012;227:1604-1609.
    PUBMED | CROSSREF

19. Kauppinen JM, Kosma VM, Soini Y, Sironen R, Nissinen M, Nykopp TK, Kärjä V, Eskelinen M, Kataja V, Mannermaa A. ST14 gene variant and decreased matriptase protein expression predict poor breast cancer survival. *Cancer Epidemiol Biomarkers Prev* 2010;19:2133-2142.
    PUBMED | CROSSREF

20. Welman A, Sproul D, Mullen P, Muir M, Kinnaird AR, Harrison DJ, Faratian D, Brunton VG, Frame MC. Diversity of matriptase expression level and function in breast cancer. *PLoS One* 2012;7:e34182.
    PUBMED | CROSSREF

21. Kim S, Yang JW, Kim C, Kim MG. Impact of suppression of tumorigenicity 14 (ST14)/serine protease 14 (Prss14) expression analysis on the prognosis and management of estrogen receptor negative breast cancer. *Oncotarget* 2016;7:34643-34663.
    PUBMED | CROSSREF

22. Zoratti GL, Tanabe LM, Varela FA, Murray AS, Bergum C, Colombo É, Lang JE, Molinolo AA, Leduc R, Marsault E, et al. Targeting matriptase in breast cancer abrogates tumour progression via impairment of stromal-epithelial growth factor signalling. *Nat Commun* 2015;6:6776.
    PUBMED | CROSSREF

23. Kim C, Lee HS, Lee D, Lee SD, Cho EG, Yang SJ, Kim SB, Park D, Kim MG. Epithin/PRSS14 proteolytically regulates angiopoietin receptor Tie2 during transendothelial migration. *Blood* 2011;117:1415-1424.
    PUBMED | CROSSREF

24. Bugge TH, Antalis TM, Wu Q. Type II transmembrane serine proteases. *J Biol Chem* 2009;284:23177-23181.
    PUBMED | CROSSREF

25. Martin CE, List K. Cell surface-anchored serine proteases in cancer progression and metastasis. *Cancer Metastasis Rev* 2019;38:357-387.
PUBMED | CROSSREF

26. Franzén O, Gan LM, Björkegren JL. PanglaoDB: a web server for exploration of mouse and human single-cell RNA sequencing data. *Database (Oxford)* 2019;2019:610-619.
PUBMED | CROSSREF

27. Geissmann F, Jung S, Littman DR. Blood monocytes consist of two principal subsets with distinct migratory properties. *Immunity* 2003;19:71-82.
PUBMED | CROSSREF

28. Palframan RT, Jung S, Cheng G, Weninger W, Luo Y, Dorf M, Littman DR, Rollins BJ, Zweerink H, Rot A, et al. Inflammatory chemokine transport and presentation in HEV: a remote control mechanism for monocyte recruitment to lymph nodes in inflamed tissues. *J Exp Med* 2001;194:1361-1373.
PUBMED | CROSSREF

29. Sunderkötter C, Nikolic T, Dillon MJ, Van Rooijen N, Stehling M, Drevets DA, Leenen PJ. Subpopulations of mouse blood monocytes differ in maturation stage and inflammatory response. *J Immunol* 2004;172:4410-4417.
PUBMED | CROSSREF

30. Wu RQ, Zhang DF, Tu E, Chen QM, Chen W. The mucosal immune system in the oral cavity-an orchestra of T cell diversity. *Int J Oral Sci* 2014;6:125-132.
PUBMED | CROSSREF

31. Jablonski KA, Amici SA, Webb LM, Ruiz-Rosado JD, Popovich PG, Partida-Sanchez S, Guerau-de-Arellano M. Novel markers to delineate murine M1 and M2 macrophages. *PLoS One* 2015;10:e0145342.
PUBMED | CROSSREF

32. Rose S, Misharin A, Perlman H. A novel Ly6C/Ly6G-based strategy to analyze the mouse splenic myeloid compartment. *Cytometry A* 2012;81A:343-350.
PUBMED | CROSSREF

33. Saja MF, Baudino L, Jackson WD, Cook HT, Malik TH, Fossati-Jimack L, Ruseva M, Pickering MC, Woollard KJ, Botto M. Triglyceride-rich lipoproteins modulate the distribution and extravasation of $Ly6C/Gr1^{low}$ monocytes. *Cell Reports* 2015;12:1802-1815.
PUBMED | CROSSREF

34. Nussbaum JC, Van Dyken SJ, von Moltke J, Cheng LE, Mohapatra A, Molofsky AB, Thornton EE, Krummel MF, Chawla A, Liang HE, et al. Type 2 innate lymphoid cells control eosinophil homeostasis. *Nature* 2013;502:245-248.
PUBMED | CROSSREF